arXiv:1207.1065v1 [hep-ph] 4 Jul 2012

Higgs boson decays to $\gamma\gamma$ and $Z\gamma$ in models with Higgs extensions

Cheng-Wei Chiang[1, 2, 3] and Kei Yagyu[1]

[1]*Department of Physics, National Central University, Chungli, Taiwan 32001, ROC*
[2]*Institute of Physics, Academia Sinica, Taipei, Taiwan 11529, ROC*
[3]*Physics Division, National Center for Theoretical Sciences, Hsinchu, Taiwan 30013, ROC*

The decays of a Higgs boson to the $\gamma\gamma$ and $Z\gamma$ final states are purely quantum mechanical phenomena that are closely related to each other. We study the effects of an extended Higgs sector on the decay rates of the two modes. We propose that a simultaneous determination of them and the ZZ mode is a useful way to see whether the Higgs boson recently observed by the LHC experiments is of the standard model type or could be a member of a larger Higgs sector.

PACS numbers:

Introduction – The quest for the origin of elementary particle masses is arguably one of the most important tasks in current high energy physics. According to the standard model (SM), a scalar field is employed to break the electroweak (EW) symmetry down to the electromagnetic (EM) symmetry, $SU(2)_L \times U(1)_Y \to U(1)_{\rm EM}$, giving masses to the W and Z bosons that mediate weak interactions. This so-called Higgs mechanism [1] is achieved when the scalar field spontaneously acquires a nonzero vacuum expectation value (VEV) due to the instability in its potential. As a consequence, the SM predicts the existence of a spin-0 Higgs boson. With the introduction of Yukawa interactions, fermionic particles can obtain their masses from the same Higgs field as well. Therefore, the discovery of the Higgs boson does not only complete the particle spectrum of the SM, but also reveals the secrets of EW symmetry breaking and mass.

Recently, both ATLAS and CMS Collaborations [2, 3] of the CERN Large Hadron Collider (LHC) have reported the observation of a Higgs boson at around 125 GeV at $\sim 5\sigma$ level through the combination of ZZ and $\gamma\gamma$ channels. Minor excesses are observed in the WW and Wh/Zh with $h \to b\bar{b}$ channels, while no excess is seen in the $\tau^+\tau^-$ channel. Around this mass region, another decay channel that is closely related to the diphoton mode and clean in the LHC environment is the $Z\gamma$ mode. At the leading order in the SM, both the $\gamma\gamma$ [4] and $Z\gamma$ [5] are loop processes mediated by the same particles. New particles beyond the SM can change their relative magnitudes. Although the ZZ decay occurs at tree level and is less sensitive to new particle contributions, the rate depends on how the EW symmetry is broken. Therefore, a simultaneous measurement of their production rates will be helpful in diagnosing the observed Higgs boson.

In view of the 125 GeV Higgs boson, denoted by h, we consider models that have only an extended Higgs sector for simplicity. There are some recent studies in the literature about the $h \to \gamma\gamma$ decay in models with an extended Higgs sector [6–8]. In this Letter, we investigate both the $h \to \gamma\gamma$ and $Z\gamma$ decays in models with Higgs extensions based on various physics motivations. We first assume that h is SM-like, meaning that the couplings of h with fermions ($h\bar{f}f$) as well as the weak gauge bosons (hVV) are the same as the SM ones. This situation can be realized by imposing a discrete Z_2 symmetry, where the SM particles are Z_2-even while the extra scalar fields are Z_2-odd. In this case, the dominant production mechanism of h at the LHC is the gluon fusion process, as in the SM. We study how the decay rates of $h \to \gamma\gamma$ and $Z\gamma$ are modified (see also [9]).

Since no excess is observed in the $h \to \tau^+\tau^-$ mode and the Wh/Zh, $h \to b\bar{b}$ decay has only a minor excess, it is still unclear whether the observed Higgs boson is SM-like. We therefore also analyze the scenario of a fermiophobic (FP) Higgs boson, in which the Yukawa couplings are vanishingly small. In this case, h is dominantly produced via the weak boson fusion process [10].

Models with a Higgs extension – In general, models with an extended Higgs sector often contain charged Higgs bosons that, among other phenomena, can contribute to the $h \to \gamma\gamma$ and $Z\gamma$ decays through the loop effect. Although there are many possibilities for the extended Higgs sector, we discuss those with extra $SU(2)_L$ singlets S (with $Y = 1$ and $Y = 2$), doublet D (with $Y = 1/2$), and triplets T (with $Y = 0$ and $Y = 1$), whose charge assignments are given in Table I [17].

We consider three distinct classes of extended Higgs sectors: (I) models with one singly-charged scalar boson, (II) those with one singly-charged and one doubly-charged scalar bosons, and (III) those with two singly-charged scalar bosons. According to the representations listed in Table I, there are three, four, and six possibilities for Class I, Class II and Class III, respectively, all listed in Table II. Examples of models in Class I (Models 1 to 3) include the two Higgs doublet model [11] and the minimal supersymmetric SM. Models in Class II (Models 4 to 7) include the Higgs triplet model [12] and Zee-Babu model [13]. Finally, models in Class III (Models 8 to 13)

	S^+	S^{++}	D	T_0	T_1
$SU(2)_L$	**1**	**1**	**2**	**3**	**3**
$U(1)_Y$	+1	+2	+1/2	0	+1

TABLE I: Charge assignments for extra scalar fields under the $SU(2)_L \times U(1)_Y$ gauge symmetry.

Model	1	2	3	4	5	6	7	8	9	10	11	12	13
S^+	1	0	0	1	0	0	0	2	0	0	1	1	1
S^{++}	0	0	0	1	0	1	1	0	0	0	0	0	0
D	0	1	0	0	0	1	0	0	2	0	1	1	0
T_0	0	0	1	0	0	0	1	0	0	2	0	0	1
T_1	0	0	0	0	1	0	0	0	0	0	0	0	0

TABLE II: Models considered in this work and their extra scalar field contents.

include those where tiny Majorana neutrino masses are generated via higher-loop processes [14].

Loop-induced diboson decays of Higgs – The decay rates of $h \to \gamma\gamma$ and $Z\gamma$ can be generally expressed as

$$\Gamma_{\gamma\gamma} = \frac{\sqrt{2}G_F\alpha_{\rm em}^2 m_h^3}{256\pi^3} \times \left|\sum_i 2Q_{S_i}^2 v\lambda_{hSS}^{ii} I_S^i + \sum_f Q_f^2 N_c^f I_f + I_W\right|^2 , \quad (1)$$

$$\Gamma_{Z\gamma} = \frac{\sqrt{2}G_F\alpha_{\rm em}^2 m_h^3}{128\pi^3}\left(1-\frac{m_Z^2}{m_h^2}\right)^3 \times \left|\sum_{i,j} 2Q_{S_i} v\lambda_{SSh}^{ij} g_{SSZ}^{ij} J_S^{ij} + \sum_f Q_f N_f^c J_f + J_W\right|^2 , \quad (2)$$

where G_F is the Fermi decay constant, $v = 1/(\sqrt{2}G_F)^{1/2}$ is the Higgs VEV, m_h is the Higgs boson mass, m_Z is the Z boson mass, Q_X is the electric charge of particle X, N_c^f is the color factor of the fermion f. The loop functions for the scalar contribution I_S^i and J_S^{ij} are given by

$$I_S^i = \frac{1}{m_h^2}[1 + 2m_{S_i}^2 C_0(0,0,m_h^2,m_{S_i},m_{S_i},m_{S_i})] ,$$

$$J_S^{ij} = \frac{1 + [m_{S_i}^2 C_0(0,m_Z^2,m_h^2,m_{S_i},m_{S_i},m_{S_j}) + (i \leftrightarrow j)]}{e(m_h^2 - m_Z^2)} + m_Z^2\frac{B_0(m_h^2,m_{S_i},m_{S_j}) - B_0(m_Z^2,m_{S_i},m_{S_j})}{e(m_h^2-m_Z^2)^2} ,$$

in terms of the Passarino-Veltman functions B_0 and C_0 defined in [15], where m_{S_i} is the mass of the charged scalar boson S_i. The loop functions for the W boson (I_W and J_W) as well as the fermion f (I_f and J_f) contributions are given in [16]. The couplings between the charged scalar bosons S_i and the Z boson as well as h are derived from

$$\mathcal{L}_S = -\lambda_{SSh}^{ij} S_i S_j^* h + i g_{SSZ}^{ij}(\partial_\mu S_i S_j^* + S_i \partial_\mu S_j^*)Z^\mu + \text{h.c.}$$

In models of Classes I and II, the couplings

$$g_{SSZ}^{ii} = \frac{g}{c_W}(I_3^i - s_W^2 Q_{S_i}),\ \lambda_{SSh}^{ii} = \frac{2}{v}(m_{S_i}^2 - M_i^2) , \quad (3)$$

where M_i is a dimensionful parameter unrelated to the Higgs VEV, I_3^i is the third isospin component of S_i, and $s_W = \sin\theta_W$, $c_W = \cos\theta_W$ with θ_W being the weak mixing angle. In Class II models, M_i for the singly-charged scalar boson ($i = 1$) and for the doubly-charged scalar boson ($i = 2$) are generally independent parameters, except for Model 5 where they are the same.

In Class III models, on the other hand, the two singly-charged charged scalar bosons $S_1^\pm$ and $S_2^\pm$ generally mix with each other, so that the expressions for g_{SSZ}^{ij} and λ_{SSh}^{ij} can be quite different from those given in Eq. (3). In this case, the coupling g_{SSZ}^{ij} are written in the mass eigenbasis of the two charged scalar bosons ($S_1^\pm, S_2^\pm$) as

$$\frac{g}{c_W}\begin{bmatrix} I_3^{\varphi_1}c_\theta^2 + I_3^{\varphi_2}s_\theta^2 - s_W^2 & (I_3^{\varphi_2} - I_3^{\varphi_1})s_\theta c_\theta \\ (I_3^{\varphi_2} - I_3^{\varphi_1})s_\theta c_\theta & I_3^{\varphi_1}s_\theta^2 + I_3^{\varphi_2}c_\theta^2 - s_W^2 \end{bmatrix} , \quad (4)$$

where θ is the mixing angle ($c_\theta = \cos\theta$, $s_\theta = \sin\theta$) connecting between the weak eigenstates ($\varphi_1^\pm$,$\varphi_2^\pm$) and the mass eigenstates: $\varphi_{1,2}^\pm = c_\theta S_{1,2}^\pm \mp s_\theta S_{2,1}^\pm$, with $I_3^{\varphi_{1,2}}$ being the third isospin component of $\varphi_{1,2}^\pm$ and $I_3^{\varphi_2} \geq I_3^{\varphi_1}$. Note that if $I_3^{\varphi_1} \neq I_3^{\varphi_2}$, the off-diagonal couplings $g_{SSZ}^{21,21}$ are nonzero and can contribute to the $h \to Z\gamma$ decay as well. λ_{SSh}^{ij} can be calculated for Models 8, 9 and 10 as

$$\lambda_{SSh}^{11,\ 22} = \frac{2}{v}(m_{S_{1,2}^+}^2 - M_{1,2}^2 c_\theta^2 - M_{2,1}^2 s_\theta^2 \mp M_3^2 s_{2\theta}) ,$$

$$\lambda_{SSh}^{12} = \frac{1}{v}\left[(M_1^2 - M_2^2)s_{2\theta} - 2M_3^2 c_{2\theta}\right] .$$

Those for Models 11 and 12 are

$$\lambda_{SSh}^{11,\ 22} = \frac{1}{v}[m_{S_{1,2}^+}^2(1 + c_{2\theta}^2) + m_{S_{2,1}^+}^2 s_{2\theta}^2 - 2M_{1,2}^2 c_\theta^2 - 2M_{2,1}^2 s_\theta^2] ,$$

$$\lambda_{SSh}^{12} = \frac{s_{2\theta}}{2v}[(m_{S_1^+}^2 - m_{S_2^+}^2)(1 - 2c_{2\theta}) + 2M_1^2 - 2M_2^2] .$$

For Model 13,

$$\lambda_{SSh}^{ii} = \frac{2}{v}(m_{S_i^+}^2 - M_i^2) ,\quad \lambda_{SSh}^{12} = 0 \ \text{ with } \ i = 1, 2 . \quad (5)$$

In the above expressions for λ_{SSh}^{ij}, the dimensionful parameters $M_{1,2,3}$ show up in the scalar potential

$$V \supset +M_1^2|\varphi_1|^2 + M_2^2|\varphi_2|^2 + M_3^2(\varphi_1^\dagger\varphi_2 + \text{h.c.}),$$

where φ_1 and φ_2 are the scalar fields including $\varphi_1^\pm$ and $\varphi_2^\pm$, respectively. In Models 11 and 12, the parameter corresponding to M_3 is absent, while there is another dimensionful parameter μ defined in the terms $\mu\Phi^\dagger\varphi_1\varphi_2 + $h.c. that induce mixing between $\varphi_1^\pm$ and $\varphi_2^\pm$, where Φ is the Higgs doublet field associated with h. In Model 13, there are no parameters corresponding to M_3 and μ and, therefore, there is no mixing at tree level.

We note in passing that the coupling formulae for λ_{SSh}^{ij} are derived assuming an unbroken discrete Z_2 symmetry in each model. If the Z_2 symmetry is broken or does not exist at all, λ_{SSh}^{ij} are generally different from those given above, even when we take the limit where h is SM-like.

Numerical results – To see the correlation between the decay rates of $h \to Z\gamma$ and $\gamma\gamma$, we further define the

Observables	Regular	FP
$\Gamma_{\rm tot}$ (MeV)	3.7	0.93
$\mathcal{B}_{\gamma\gamma}$ (%)	0.28	1.8
$\mathcal{B}_{Z\gamma}$ (%)	0.18	0.79
$\mathcal{B}_{ZZ}$ (%)	2.3	9.1
$R = \Gamma_{Z\gamma}/\Gamma_{\gamma\gamma}$	0.63	0.43

TABLE III: Total decay rate and branching ratios of a regular and FP Higgs boson, respectively, in the SM.

Model	1	2	3	
$\Delta\mathcal{B}_{\gamma\gamma}$ (%)	−9.9 (4.2)	−9.9 (4.2)	−9.9 (4.2)	
$\Delta\mathcal{B}_{Z\gamma}$ (%)	3.3 (−1.2)	−3.8 (1.4)	−11 (4.2)	
R	0.72 (0.60)	0.67 (0.61)	0.63 (0.63)	
Model	**4**	**5**	**6**	**7**
$\Delta\mathcal{B}_{\gamma\gamma}$ (%)	−45 (11)	−45 (11)	−45 (11)	−45 (11)
$\Delta\mathcal{B}_{Z\gamma}$ (%)	17 (−3.4)	−12 (2.5)	9.4 (−1.9)	2.2 (−0.50)
R	1.3 (0.55)	1.0 (0.58)	1.3 (0.56)	1.2 (0.56)

TABLE IV: Deviations of the $h \to \gamma\gamma$ and $Z\gamma$ branching ratios from the SM expectations and the ratio R in models of Classes I and II. All the charged scalar boson masses are taken to be 400 GeV. The numbers without (with) parentheses correspond to the case with $M = 0$ ($M = M_{\rm MAX}$), where $M_{\rm MAX}$ denotes the maximum value allowed by the conditions in Eqs. (6) and (7). In Class I models $M_{\rm MAX} = 470$ GeV, while in Class II models $M_{\rm MAX} = 440$ GeV assuming $M_1 = M_2 = M$.

Model (FP)	1	2	3	
$\Delta\mathcal{B}_{\gamma\gamma}$ (%)	500 (570)	500 (570)	500 (570)	
$\Delta\mathcal{B}_{Z\gamma}$ (%)	360 (340)	330 (350)	300 (360)	
R	0.48 (0.41)	0.45 (0.42)	0.42 (0.43)	
Model (FP)	**4**	**5**	**6**	**7**
$\Delta\mathcal{B}_{\gamma\gamma}$ (%)	320 (610)	320 (610)	320 (610)	320 (610)
$\Delta\mathcal{B}_{Z\gamma}$ (%)	410 (330)	290 (350)	380 (330)	350 (340)
R	0.78 (0.38)	0.60 (0.40)	0.73 (0.39)	0.69 (0.39)

TABLE V: Same as Table IV, but for the FP Higgs case.

ratio $R \equiv \Gamma_{Z\gamma}/\Gamma_{\gamma\gamma}$. First, we give the SM expectations of the two diboson decays of a regular and FP Higgs boson in Table III, where $m_h = 125$ GeV and $m_t = 173$ GeV are used. Next, we show numerical results for the case with an extended Higgs sector. As mentioned before, we assume that the observed Higgs boson is SM-like in couplings with the gauge bosons and fermions in our numerical studies. Moreover, we present the results for the case where the charged scalar boson are at least 400 GeV in mass.

For meaningful discussions, we calculate parameter bounds by considering unitarity and vacuum stability constraints. For unitarity, we impose the condition that the magnitudes of all dimensionless coupling constants do not exceed 2π. For vacuum stability, we require that the scalar potential is bounded from below in the parameter space where the quartic terms dominate. Combining the two bounds, we obtain the following conditions for Classes I, II and III, respectively:

$$-\frac{m_h}{v} < \frac{m_S^2 - M^2}{\sqrt{\pi}v^2} < \sqrt{\pi}\ , \tag{6}$$

$$-\frac{m_h}{\sqrt{2}v} < \frac{m_{S_{1,2}}^2 - M_{1,2}^2}{\sqrt{\pi}v^2} < \sqrt{\pi}\ , \tag{7}$$

$$-\frac{m_h}{\sqrt{2}v} < \frac{m_{S_{1,2}}^2 c_\theta^2 + m_{S_{2,1}}^2 s_\theta^2 - M_{1,2}^2}{\sqrt{\pi}v^2} < \sqrt{\pi}\ . \tag{8}$$

We shall use them and neglect the slight changes among the models in each class due to some coupling constants that are irrelevant to our analysis.

The deviations from the SM predictions for the $h \to \gamma\gamma$ and $Z\gamma$ branching ratios can be parametrized as

$$\Delta\mathcal{B}_{\gamma\gamma(Z\gamma)} = \left[\mathcal{B}^{\rm NP}_{\gamma\gamma(Z\gamma)} - \mathcal{B}^{\rm SM}_{\gamma\gamma(Z\gamma)}\right] / \mathcal{B}^{\rm SM}_{\gamma\gamma(Z\gamma)}\ , \tag{9}$$

where $\mathcal{B}^{\rm NP}_{\gamma\gamma}$ ($\mathcal{B}^{\rm NP}_{Z\gamma}$) is the branching ratio of $h \to \gamma\gamma$ ($h \to Z\gamma$) in a Higgs-extended model, while $\mathcal{B}^{\rm SM}_{\gamma\gamma}$ ($\mathcal{B}^{\rm SM}_{Z\gamma}$) is that in the SM. In Table IV, the deviations and R are listed in the case of $m_{S^+} = 400$ GeV for Class I models, and $m_{S^+} = m_{S^{++}} = 400$ GeV with $M_1 = M_2 = M$ for Class II models. The parameter M is constrained by Eqs. (6) and (7) to be $0 < M \lesssim 470$ (440) GeV for Class I (Class II). The results for the FP Higgs boson scenario using the same parameter set are given in Table V.

For models in Class III, we consider as an example the case where $m_{S_1^+} = 400$ GeV and $m_{S_2^+} = 500$ GeV. We assume that the three dimensionful parameters are the same: $M_1 = M_2 = M_3 = M$. The maximally allowed value of M depends on the mixing angle θ, but the strictest upper bound on M from Eq. (8) is found when $\theta = 0$. In this case, the upper bound is 440 GeV, which is used in the following numerical analysis.

In Fig. 1, the deviation of the $h \to \gamma\gamma$ branching ratio is plotted against $\sin\theta$. According to the left plot for the scenario with a regular Higgs boson, Models 8 − 10 all have the same behavior of positive corrections, while Models 11 and 12 share a common negative corrections. Model 13, on the other hand, is a constant due to Eq. (5) and has virtually no deviation from the SM expectation. In the scenario with an FP Higgs, however, the deviations are all shifted to around +550% or more.

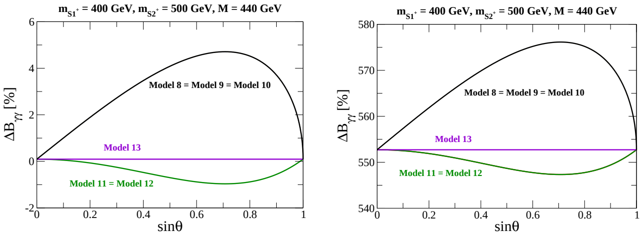

FIG. 1: Deviation of the branching ratio of $h \to \gamma\gamma$ as a function of $\sin\theta$. We take $M_1 = M_2 = M_3 = M = 440$ GeV, $m_{S_1^+} = 400$ GeV and $m_{S_2^+} = 500$ GeV. The left (right) figure shows the case with the regular (FP) Higgs boson.

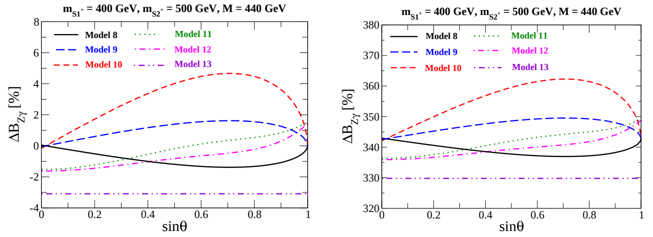

FIG. 2: Deviation of the branching ratio of $h \to Z\gamma$ as a function of $\sin\theta$. We take $M_1 = M_2 = M_3 = M = 440$ GeV, $m_{S_1^+} = 400$ GeV and $m_{S_2^+} = 500$ GeV. The left (right) figure shows the case with the regular (FP) Higgs boson.

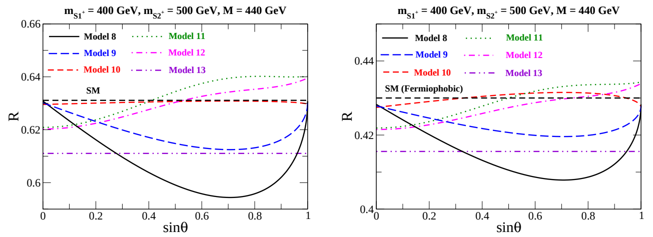

FIG. 3: The ratio R as a function of $\sin\theta$. We take $M_1 = M_2 = M_3 = M = 440$ GeV, $m_{S_1^+} = 400$ GeV and $m_{S_2^+} = 500$ GeV. The left (right) figure shows the case with the regular (FP) Higgs boson. The SM case is indicated by the dashed line for comparison.

The deviation of the $h \to Z\gamma$ branching ratio varies a lot among the Class III models, as shown in Fig. 2. For the scenario with a regular (FP) Higgs boson, the deviation is between about -3% and 5% (330% and 360%). Finally, we show the ratio R in Fig. 3 for the two scenarios as well, in contrast with the values for the SM.

We now briefly comment on the case with lighter charged scalar bosons. When we take all their masses to be 200 GeV and use the maximally allowed M, the deviation in the branching ratio of $h \to \gamma\gamma$ is predicted to be 14 %, 59% and 22% in Classes I, II and III with $\theta = 0$, respectively, in the regular Higgs boson scenario.

Summary – With the observation of a Higgs boson h of mass 125 GeV by ATLAS and CMS, it would be interesting to diagnose whether h is standard model-like (SM-like) or part of a larger Higgs sector. We thus consider and classify models with simple Higgs extensions. We have imposed the unitarity and vacuum stability constraints on the model parameters. We have studied the neutral diboson decays of h, assuming that it has SM-like couplings with the weak bosons and fermions. In our framework, the ZZ mode is virtually unaffected, whereas the $\gamma\gamma$ and $Z\gamma$ modes can be modified by a few to a few tens of percent. A simultaneous determination of their branching ratios is thus useful in exploring the possibility of an extended Higgs sector. As a comparison, we have also considered the scenario where h is fermiophobic and observed more dramatic changes in the diboson decay rates.

Acknowledgments The authors thanks C. M. Kuo for useful discussions. This research was supported in part by the National Science Council of Taiwan, R. O. C.

[1] F. Englert and R. Brout, Phys. Rev. Lett. **13**, 321 (1964); P. W. Higgs, Phys. Rev. Lett. **13**, 508 (1964); G. S. Guralnik, C. R. Hagen and T. W. B. Kibble, Phys. Rev. Lett. **13**, 585 (1964).

[2] F. Gianotti, talk presented at the CERN seminar, Geneva, Switzerland, July 4, 2012.

[3] J. Incandela, talk presented at the CERN seminar, Geneva, Switzerland, July 4, 2012.

[4] J. R. Ellis, M. K. Gaillard and D. V. Nanopoulos, Nucl. Phys. B **106**, 292 (1976); B. L. Ioffe and V. A. Khoze, Sov. J. Part. Nucl. **9**, 50 (1978) [Fiz. Elem. Chast. Atom. Yadra **9**, 118 (1978)]; M. A. Shifman, A. I. Vainshtein, M. B. Voloshin and V. I. Zakharov, Sov. J. Nucl. Phys. **30**, 711 (1979) [Yad. Fiz. **30**, 1368 (1979)].

[5] R. N. Cahn, M. S. Chanowitz and N. Fleishon, Phys. Lett. B **82**, 113 (1979); L. Bergstrom and G. Hulth, Nucl. Phys. B **259**, 137 (1985).

[6] P. Posch, Phys. Lett. B **696**, 447 (2011); A. Arhrib, R. Benbrik and N. Gaur, Phys. Rev. D **85**, 095021 (2012); P. M. Ferreira, R. Santos, M. Sher and J. P. Silva, Phys. Rev. D **85**, 035020 (2012).

[7] A. Arhrib, R. Benbrik, M. Chabab, G. Moultaka and L. Rahili, JHEP **1204**, 136 (2012); S. Kanemura and K. Yagyu, Phys. Rev. D **85**, 115009 (2012).

[8] S. Kanemura, T. Kasai, G. -L. Lin, Y. Okada, J. -J. Tseng and C. P. Yuan, Phys. Rev. D **64**, 053007 (2001).

[9] M. Carena, I. Low and C. E. M. Wagner, arXiv:1206.1082 [hep-ph].

[10] E. Gabrielli, B. Mele and M. Raidal, arXiv:1202.1796 [hep-ph].

[11] M. Sher, Phys. Rept. **179**, 273 (1989); G. C. Branco, P. M. Ferreira, L. Lavoura, M. N. Rebelo, M. Sher and J. P. Silva, Phys. Rept. **516**, 1 (2012).

[12] T. P. Cheng and L. F. Li, Phys. Rev. D **22**, 2860 (1980); J. Schechter and J. W. F. Valle, Phys. Rev. D **22**, 2227 (1980).

[13] A. Zee, Nucl. Phys. B **264**, 99 (1986); K. S. Babu, Phys. Lett. B **203**, 132 (1988).

[14] A. Zee, Phys. Lett. B **93**, 389 (1980); A. Zee, Phys. Lett. B **161**, 141 (1985); L. M. Krauss, S. Nasri and M. Trodden, Phys. Rev. D **67**, 085002 (2003); M. Aoki, S. Kanemura and O. Seto, Phys. Rev. Lett. **102**, 051805 (2009).

[15] G. Passarino and M. J. G. Veltman, Nucl. Phys. B **160**, 151 (1979).

[16] A. Djouadi, Phys. Rept. **457**, 1 (2008).

[17] The scalar doublet field with $Y = 3/2$ does not contain a neutral component, and cannot couple to the other SM particles at tree level if no other particles are introduced. Therefore, we do not consider such a case.